Electronic Supplementary Material (ESI) for Physical Chemistry Chemical Physics.
This journal is © the Owner Societies 2019

Supporting Information

Dependence of Water Adsorption on Surface Structure of Silicon Wafer Aged in Different Environmental Conditions

Lei Chen[a], Dien Ngo[b], Jiawei Luo[b], Yunfei Gong[a], Chen Xiao[a], Xin He[b], Bingjun Yu[a], Linmao Qian[a,*], and Seong H. Kim[a,b,*]

[a] Tribology Research Institute, State Key Laboratory of Traction Power, Southwest Jiaotong University, Chengdu 610031, China

[b] Department of Chemical Engineering and Materials Research Institute, The Pennsylvania State University, University Park, Pennsylvania 16802, USA

E-mail: linmao@swjtu.edu.cn; shkim@engr.psu.edu

I. XPS measurements on a pristine Si/H surface and other aged Si surfaces

The surface oxidation state of a pristine Si/H surface was analyzed using X-ray photoelectron spectroscopy (XPS; XSAM 800, KRATOS, Inc., England). Fig. S1 shows the Si 2p XPS spectrum of the Si/H surface. The peak at 99.15 eV is the Si bulk (Si^0).[1] No obvious peak at 102.9 eV (below detection limit of XPS) corresponding to Si-O in native oxide layer indicates that all native oxide layers have been removed.

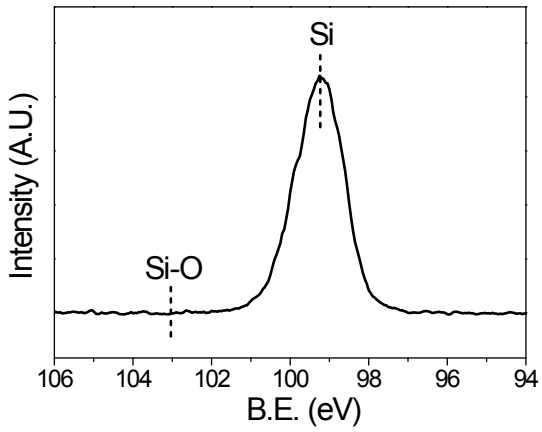

Fig. S1 Si 2p XPS spectrum of a pristine Si/H surface.

Fig. S2 compares the high-resolution Si 2p spectra of the Si_{water}, Si_{air} and $Si_{alcohol}$ surfaces aged for 14 days and 28 days. The bulk silicon peak is at 99.15 eV and the oxidized silicon (Si-O) is at 102.9 eV. The Si-O peak area normalized to the Si peak area ($A_{Si\text{-}O}/A_{Si}$) as a function of aging time in three environments is plotted in Fig. S2d. In the case of aging in air (Si_{air}), the $A_{Si\text{-}O}/A_{Si}$ ratio reaches about 0.1. In comparison, the $A_{Si\text{-}O}/A_{Si}$ ratio increases quickly to ~0.21 and then stays constant for the Si_{water} case, while it increases gradually to ~0.05 for the $Si_{alcohol}$ case. This means that liquid water environment is much more oxidative than air, while the liquid ethanol environment is less oxidative than air.

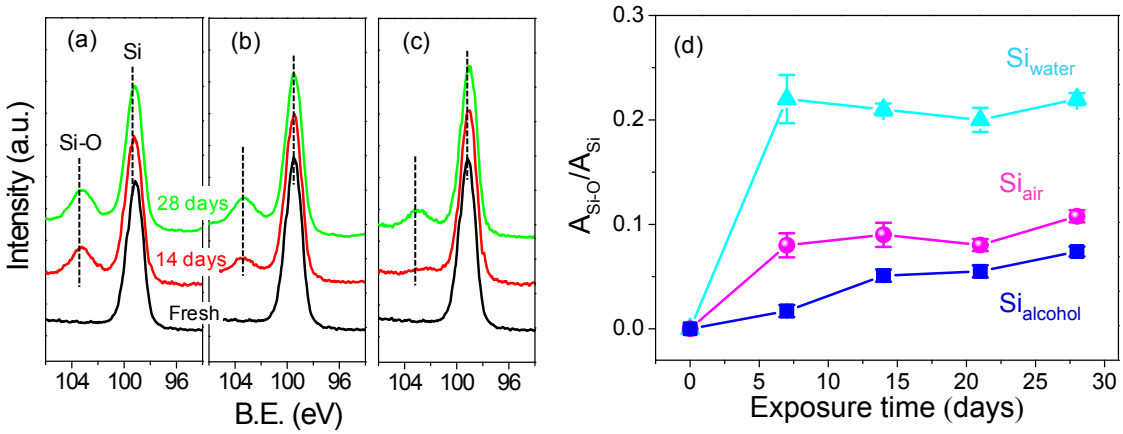

Fig. S2 Si 2p narrow XPS spectra of H/Si surface after storing for various times in DI water (a), air (b), and liquid alcohol (c). (d) Normalized area of the Si-O peak ($A_{Si\text{-}O}/A_{Si}$) as a function of exposure time (*days*) in liquid alcohol, air, and DI water.

II. Topography of hydrogen-terminated Si surfaces before and after aging in various environments

The topographies of the Si wafers treated in different environments were characterized using Atomic Force Microscopy (AFM, SPI3800N, Seiko, Japan) with a Si_3N_4 probe (MLCT, Veeco, USA) with a nominal radius (*R*) of ~15 nm. Fig. S3 compares the AFM images of a pristine hydrogen-terminated Si (Si/H) surface before and after aging for 28 days in liquid water (Si_{water}), air (~35% relative humidity, Si_{air}) and liquid alcohol ($Si_{alcohol}$). The root-mean-squares (RMS) roughness on a scan area of 1 × 1 μm^2 is calculated to be ~0.1 nm on the pristine Si/H surface (Fig. S3a), and it finally increases to ~0.25 nm on Si_{water} surface (Fig. S3b) and

~0.13 nm on Si_{air} surface (Fig. S3c), respectively. In contrast, no discernable change is observed on the $Si_{alcohol}$ surface (Fig. S3d).

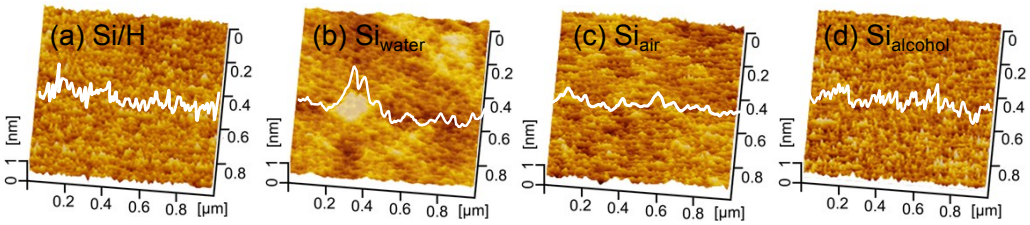

Fig. S3 AFM images of (a) Si/H surface, (b) Si_{water}, (c) Si_{air}, and (d) $Si_{alcohol}$ surfaces after aging for 28 days in corresponding environments. The white lines are the cross-section profiles of topography measured on the middle location. All profile lines are at the same scale and the maximum height of the profile line in (b) is ~1.5 nm. The areas of 1 × 1 μm^2 are scanned using a sharp Si_3N_4 tip with a radius of ~ 15 nm.

III. SE data analysis

The SE analysis of samples in this study was performed on a rotating compensator spectroscopic ellipsometer (J.A. Woollam Co. Alpha-SE).[2] The measured spectra of aged samples were fitted to an optical model consisting of a silicon substrate, a native oxide layer and an artificial layer. The artificial layer was used to account for surface roughness of samples and surface contamination. Fig. S4 shows the experimental data, SE fittings, and optical model for a fresh Si/H surface. The SE data were fitted well when the oxide layer was set to zero and the artificial layer was modeled to consist of 50% silicon and 50% void.[2]

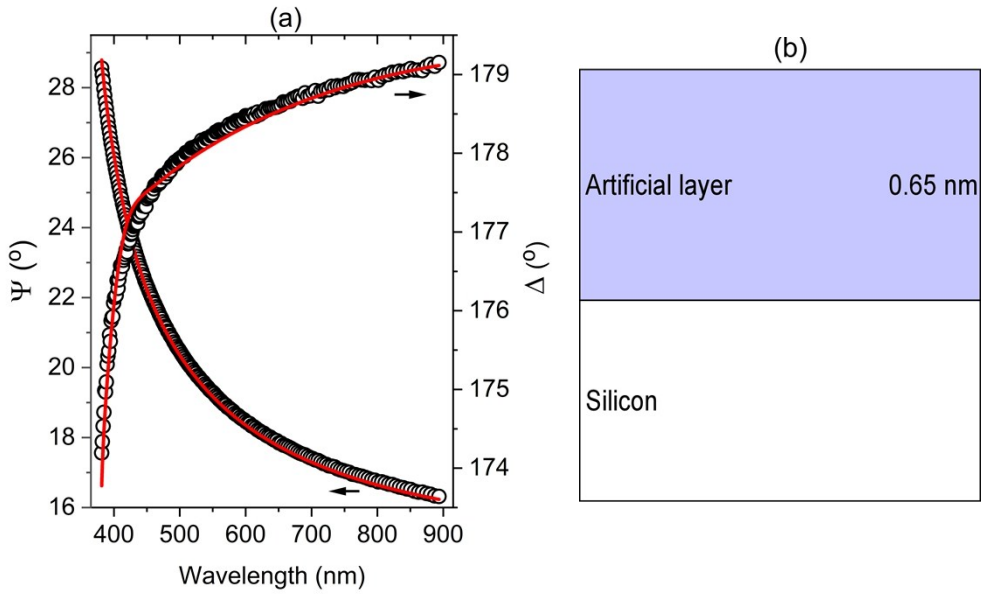

Fig. S4 Spectroscopic ellipsometry of a fresh Si/H sample: (a) experimental data (open circles) and SE fittings (solid lines); (b) optical model.

IV. Pull-off measurements on Si/H, Si_{water}, Si_{air} and $Si_{alcohol}$ surfaces

The pull-off measurements were conducted in liquid water using AFM and a Si_3N_4 probe with a nominal radius of ~15 nm. Fig. S5 compares the typical force-displacement curves observed for the pristine Si/H surface and the 28-day aged $Si_{alcohol}$, Si_{air}, and Si_{water} surfaces. For the Si/H, $Si_{alcohol}$, and Si_{air} surfaces, a clean single snap-off peak is detected. In contrast, the Si_{water} surface shows multiple pull-off snaps with extremely small forces. This behavior is somewhat similar to the cases observed in the pull-off measurements of chain-like DNA and other polymer films.[3-5] This difference clearly suggests that the oxidized layer on Si_{water} might have swellable polymer-like chains, which are not observed for the native oxide layer on Si_{air} and $Si_{alcohol}$ surfaces. Knowing that rinsing the solvent-cleaned oxide surface in water is a good way of preventing deposition of organic residue onto the surface,[6] it is unlikely that such polymer-like chains are from contaminants from water. They must be the product of oxidative reactions of silicon with water.

Fig. S5 Comparison of the force-displacement curves measured for (a) Si/H, (b) $Si_{alcohol}$, (c) Si_{air}, and (d)

Si_{water} with a sharp Si_3N_4 AFM tip (radius ~15 nm) in liquid water. The aging times for the (b-d) samples are 28 days. (e) Enlarged plot of the snap-off region of the data in (d).

V. Degradation the Si/H surface in liquid water

Fig. S6a shows the ATR-IR spectra of the Si_{water} surface in the range from 2020 cm^{-1} to 2170 cm^{-1} in which the peak is attributed to the Si-H stretching modes.[9,10] Along with the aging in liquid water, the area of the Si-H peak decreases gradually. Fig. S6b demonstrates that, with the increase in aging time, the integrated peak area decreases sharply to a constant value after a critical aging time.

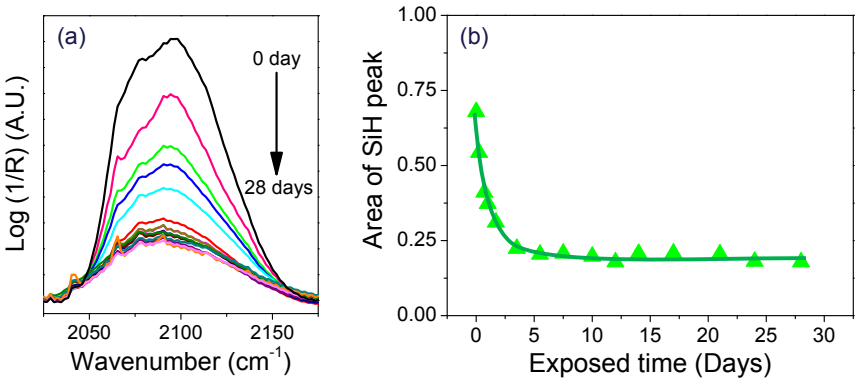

Fig. S6 Evolution of silane (SiH) groups on Si/H surface exposed in DI water. (a) ATR-IR spectra of surface silane groups on the Si-H surface as the exposing time increases from 0 day to 28 days. (b) Integrated area of SiH peak in (a) as a function of exposing time.

VI. Evolution of water adsorption on Si_{water} surface with the aging time

The ATR-IR spectra of adsorbed water layers measured during the step-wise increase of aging time from 0.25 to 28 days on the Si_{water} surfaces are reported in Fig. S7. The hydrogen-bonding interactions of water due to O-H stretching result in the occurrence of the peaks in the range from 3000 cm^{-1} to 3800 cm^{-1}, which can be fitted with two main components, including the strongly hydrogen-bonded configuration (ice-like) at 3220 cm^{-1} (peak-I) and the weakly hydrogen-bonded configuration (liquid-like) at 3400 cm^{-1} (peak-II).[11,12] During the data fitting process, the centers of the peak 1 and peak 2 were fixed (Fig. S7) and their full width at half-

maximum (FWHM) were allowed to vary but did not change much (Fig. S8).

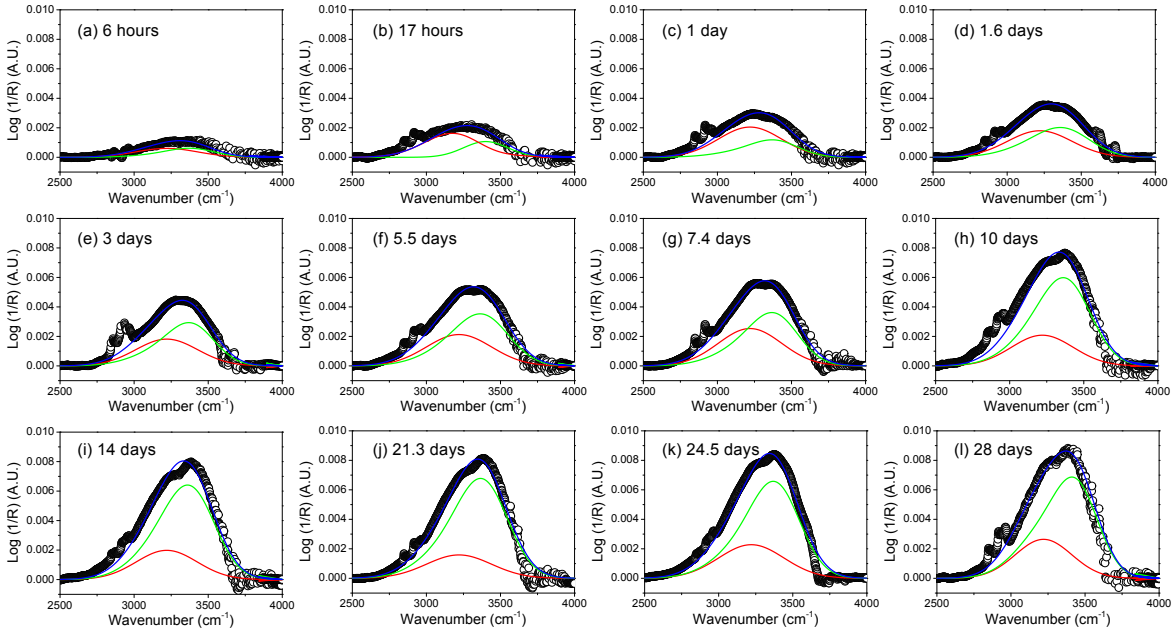

Fig. S7 ATR-IR spectra of the O-H stretching region of water adsorbed on Si_{water} surface as the aging time in DI water increases from 0.25 days to 28 days. All spectra could be fitted with two components – peak-I (clear red curve centered at 3220 cm^{-1}) and peak-II (green line shaped based on the ATR-IR spectrum of liquid water). The relative humidity for all measurements was controlled around 35 ± 5%.

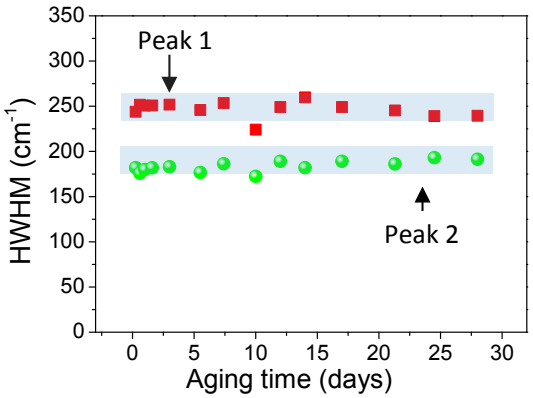

Fig. S8 Full width at half-maximum (FWHM) of the peak 1 and peak 2 in the ATR-IR spectra shown in Fig. S7.

VII. Estimation of the adsorbed water thickness

Based on the obtained ATR-IR spectra, the thickness of the adsorbed water layer (d) can be estimated by comparing the integrated areas of adsorbed species (A_{ads}) with the integrated area of bulk water (A_{bulk}, Fig. 4d) with consideration of the penetration depth of the squared IR evanescent field (d_{bulk} / 2) ,[13]

$$d = \frac{A_{ads}}{A_{bulk}}(d_{bulk}/2) = \frac{A_{ads}}{A_{bulk}} \frac{\lambda}{4\pi(n_1^2 \sin^2\theta - n_2^2)^{1/2}} \quad \text{(S1)}$$

where λ is the wavelength of IR, θ is the incident angle of the IR beam (45°). n_1 and n_2 are the refractive indices of the substrate and bulk water, respectively. The d_{bulk} of liquid water is defined as the depth where the evanescent field intensity decreases to e^{-1}, which is very close to the depth where the integrated area of the evanescent field from the surface is a half of the total integrated area. Thus, the ATR-IR intensity of bulk water can be considered as that of a water film with the thickness of d_{bulk} / 2. The ATR-IR results shown in Fig. 3 in the main text and Fig. S8 indicate that the adsorbed water layer consists of ordered component (peak-I) and disordered component (peak-II). Then, the total thickness (d) can be expressed as the sum of the thicknesses of ordered water ($d_{ordered}$) and disordered water ($d_{disordered}$). The thickness of each component can be estimated by Eq. S1 with the refractive index of bulk ice (n_2=1.30) and the area of peak-I for $d_{ordered}$; and the refractive index of bulk liquid (n_2=1.33) and the area of peak-II for $d_{disordered}$.[14,15] More details about the thickness estimation of adsorbed water layer have been reported in ref. 13.

References

1. Maccarini, M.; Himmelhaus, M.; Stoycheva, S.; Grunz, M. *Appl. Surf. Sci.* **2005**, *252*, 1941-1946.
2. Ngo, D.; Liu, H.; Sheth, N.; Lopez-Hallman, R.; Podraza, N. J.; Collin, M.; Gin, S.; Kim, S. H. *NPJ Materials Degradation* **2018**, *2* (1), 20.
3. Wang, M.; Cui, S. X.; Yu, B. J.; Qian, L. M. *Sci. China: Technol. Sci.* **2013**, *56(12)*, 2927-2933.
4. Kim, S. H.; Opdahl, A.; Marmo, C.; Somorjai, G. A. *Biomaterials* **2002**, *23*, 1657-1666.
5. Hugel, T.; Seitz, M. *Rapid Commun.* **2001**, *22*, 989-1016.
6. Barthel, A. J.; Luo, J. W.; Hwang, K. S.; Lee, J. Y.; Kim, K. S. *Wear* **2016**, *350*, 21-26.
7. Horsthemke, A.; Schroder, J. J. *Chem. Eng. Process.* **1985**, *19*, 277-285.
8. Williams, D. L.; Mittal, K. L. Wettability Techniques to Monitor the Cleanliness of Surfaces, In R. Kohli &

K.L. Mittal (Eds): Developments in Surface Contamination and Cleaning; Elsevier: Amsterdam, 2016.

9. Takahagi, T.; Nagai, I.; Ishitani, A.; Kuroda, H.; Nagasawa, Y. *J. Appl. Phys.* **1988**, *64*, 3516.
10. Chabal, Y. J.; Higashi, G. S.; Raghavachari, K. *J. Vac. Sci. Technol. A* **1998**, *7*, 2104.
11. Scherer, J. R. Advances in Infrared and Raman Spectroscopy; Heyden: London, 1978.
12. Ewing, G. E. *J. Phys. Chem. B* **2004**, *108*, 15953.
13. Barnette, A. L.; Kim, S. H. *J. Phys. Chem. C* **2012**, *116*, 9909-9916.
14. Warren, S. G. *Appl. Optics* **1984**, *23(8)*, 1206-1225.
15. Daimon, M.; Masumura, A. *Appl. Optics* **2007**, *46(18)*, 3811-3820.